Detection of kiwifruit dry matter content based on hyperspectral technology using uninformed variable elimination coupled with successive projection algorithm

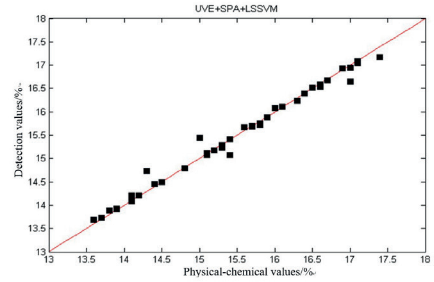

Detección del contenido de materia seca de los kiwis basada en la tecnología hiperespectral mediante la eliminación de variables no informadas (UVA) junto con un algoritmo de proyección sucesiva (SPA)

Lijia Xu[1], Lina Zheng[1],Peng Huang[1*],Heng Chen1 and Zhiliang Kang[2]

[1] College of Mechanical and Electrical Engineering, Sichuan Agricultural University, Ya'an, 625014, China
[2] School of physics and Electrical Engineering, Liupanshui Normal University, Liupanshui, 553000, China
* Corresponding Author, E-mail: hpsjdyd@qq.com

DOI: http://dx.doi.org/10.6036/9837 | Recibido: 09/04/2020 • Inicio Evaluación: 09/04/2020 • Aceptado: 30/07/2020

RESUMEN

- Los parámetros internos de los kiwis se detectan en su mayoría mediante métodos físico-químicos destructivos tradicionales, que no sólo consumen mano de obra y tiempo, sino que también son inconvenientes en su funcionamiento. La técnica de imágenes hiperespectrales se considera ahora un nuevo método no destructivo para detectar los parámetros de calidad de los kiwis. Sin embargo, la mayoría de los estudios se centraron en la detección del contenido de sólidos solubles, la dureza y la madurez de esta fruta. Por lo tanto, es necesario mejorar la precisión de la detección de esta técnica de imágenes. Además, pocas de estas técnicas están involucradas en la detección del contenido de materia seca. En este estudio se propone un método de detección no destructivo basado en la técnica de imágenes hiperespectrales para detectar el contenido de materia seca de los kiwis en línea de manera rápida y precisa. En primer lugar, se analizaron las imágenes hiperespectrales de los kiwis, se extrajeron las regiones interesadas en ellos y se preprocesó la eliminación de ruidos mediante la corrección de dispersión multiplicativa. En segundo lugar, se investigó la redundancia de las 217 piezas de información espectral de banda completa, y 66 bandas espectrales características fueron inicialmente eliminadas a través de la eliminación de variables no informadas (UVE). La colinealidad entre estas bandas se eliminó mediante el algoritmo de proyección sucesiva (SPA), y se extrajeron cinco bandas espectrales características. Por último, se detectó el contenido de materia seca del kiwi tomando como detector el vector de soporte de mínimos cuadrados (LSSVM), empleando la optimización del enjambre de partículas (PSO) para optimizar los parámetros del LSSVM, e introduciendo las cinco bandas en el LSSVM posteriormente. Los resultados de las pruebas muestran que: 1) la redundancia y la colinealidad de las bandas espectrales completas pueden eliminarse eficazmente combinando el SPA con el UVE, de modo que las bandas espectrales características de baja dimensión extraídas puedan reflejar mejor el contenido de materia seca del kiwi. 2) Los indicadores de detección de UVE+SPA+LSSVM al conjunto de formación es que el coeficiente de correlación (R) = 0,91, el error cuadrático medio de la raíz (RMSE) = 0,28, y los indicadores de detección al conjunto de predicción es que R = 0,89, RMSE = 0,31, lo que indica que la precisión de la detección es mayor que la de los otros métodos. Este estudio muestra que el método de detección no destructivo propuesto en este documento puede detectar el contenido de materia seca del kiwi de manera rápida y eficiente. Este método sirve de base teórica para la clasificación industrializada del kiwi que se basa en los parámetros internos.
- **Palabras clave:** Contenido de materia seca, Eliminación variable no informada (UVE), Algoritmo de proyección sucesiva (SPA), Máquina vectorial de soporte de mínimos cuadrados (LSSVM).

ABSTRACT

The internal parameters of kiwifruit are mostly detected using traditional destructive physical–chemical methods, which are not only labor and time consuming but also inconvenient in operation. The hyperspectral imaging technique is now considered a new non-destructive method for detecting the quality parameters of kiwifruits. However, most studies focused on detecting the soluble solid content, hardness, and ripeness of this fruit. Thus, the detection precision of this imaging technique needs to be improved. Moreover, few of these techniques are involved in the detection of the dry matter content. A non-destructive detection method based on the hyperspectral imaging technique is proposed in this study to detect the dry matter content of kiwifruit online rapidly and precisely. First, the hyperspectral images of kiwifruit were analyzed, the interested regions therein were extracted, and denoising was preprocessed using the multiplicative scatter correction. Second, the redundancy of the 217 pieces of full-band spectral information was researched, and 66 characteristic spectral bands were initially screened out through uninformed variable elimination (UVE). The collinearity among these bands was eliminated using successive projection algorithm (SPA), and five characteristic spectral bands were extracted. Finally, the dry matter content of the kiwifruit was detected by taking least squares support vector (LSSVM) as the detector, by employing particle swarm optimization (PSO) to optimize LSSVM's parameters, and by entering the five bands into the LSSVM later. Test results show that: (1) the redundancy and the collinearity of the full spectral bands can be eliminated effectively by combining SPA with UVE so that the extracted low-dimensional characteristic spectral bands can reflect the dry matter content of kiwifruit better. (2) The detection indicators of UVE+SPA+LSSVM to the training set is that the coefficient of correlation (R) = 0.91, root-mean-square error (RMSE) = 0.28, and the detection indicators to the prediction set is that R = 0.89, RMSE = 0.31, indicating that the detection precision is higher than the other methods. This study shows that the non-destructive detection method proposed in this paper can detect the dry matter content of kiwifruit rapidly and efficiently. This method serves as a theoretical basis for the industrialized classification of kiwifruit that is based on the internal parameters.

Keywords: Dry matter content, Uninformed variable elimination (UVE), Successive projection algorithm (SPA), Least squares support vector machine (LSSVM).

1. INTRODUCTION

China is a major kiwifruit planting and exporting country in the world. Kiwifruit, also known as the "King of Fruits," is rich in fructose, vitamin C, gluconic acid, citric acid, and other substances [1-2]. The quality of the internal parameters of kiwifruit affects the taste of kiwifruit directly, thereby also affecting the export of Chinese kiwifruit. In recent years, machine vision based non-destructive detection techniques have been mainly used to determine the external characteristics of farm products, such as size, shape, color, and surface defects. Although the non-destructive detection that aims at the internal parameters of farm products has drawn extensive attention of scholars at home and abroad reports on the non-destructive detection of parameters, such as the soluble solid content (SSC), maturity, and dry matter (DM) of kiwifruit, are few. The measured internal parameters of kiwifruit are conducive to the classified sales of kiwifruit. The internal parameters of the kiwifruit measured by sampling can also be used to guide the cultivation method and management process of fruit farmers and determine the picking and storage times of the kiwifruit to improve the economic benefits of fruit farmers. At present, the internal parameters of kiwifruit are commonly detected using traditional physical–chemical methods, which are laborious, cumbersome, and time-consuming. Such methods also involve destructive sampling detection to kiwifruit. In recent years, research advances in the non-destructive testing of the internal parameters of agricultural products have been reported [3-5], of which the hyperspectral imaging technique [6] is a widely applied multinarrow band-based imaging data technique. This technique utilizes electromagnetic spectrum to research the spectral characteristics of various kinds of matter in the form of image, thereby allowing the detection of the internal and external characteristic parameters of the samples.

A series of findings have been made in the studies on non-destructive detection for the internal parameters of farm products [7-9]. Although SSC and DM are important internal parameters of kiwifruit, most studies focus on the detection of SSC. SSC is the general term of all water soluble compounds in kiwifruit, including sugar, acid, vitamins, etc, while DM is the comprehensive index to measure the accumulation of organic matter and the amount of nutrients in kiwifruit. Usually, the higher the SSC, the better the maturity of kiwifruit, while the higher the DM, the better the quality of kiwifruit. Generally, kiwifruit is fully dried at a given constant temperature, and the weight of the remaining organic matter is taken as its DM value, but this method is time-consuming, laborious and not practical. Therefore, it is necessary to propose an effective non-destructive detection method for the DM of kiwifruit. The DM of kiwifruit is rich in organic matters, such as C-H, O-H, N-H, and other organic chemical bonds, which can be taken as spectral sensitive radical groups. The DM can be reflected by the absorbing capacity of the spectral sensitive radical groups. Thus, designing a suitable characteristic extracting method is necessary hereto. This study intends to design a non-destructive DM detection method that is based on hyper-spectral imaging technique[10] for specific varieties of kiwifruit to research its spectral band pre-denoising and the extraction of the corresponding characteristic spectrum intensively, analyze the relationship between the characteristic of the spectral bands and the DM of kiwifruit, and select an appropriate detector to identify the DM.

2. START OF THE ART

To date, many research on the detection of the internal parameters of kiwifruit, apples, and other fruits have been performed by scholars at home and overseas using infrared-spectrum or hyper-spectrum technique. LI et al. [11] established SSC and hardness detection models for kiwifruit with partial least squares (PLS) and support vector machine (SVM) and took visible-near infrared spectral images as input. The test result showed that the detection performance of SVM is slightly superior to that of PLS but with low detection precision. MCGLONE et al. [12] acquired visible-IR spectral images within the band range of 300–1140 nm and detected the DM and SSC of yellow-flesh kiwifruit by using PLS. The RMSEs that corresponded with the prediction set were 0.40 and 0.71, respectively. Thus, detection precision needs to be improved. LI et al. [13] acquired spectral images within the band range of 898.27–1719.61nm and corrected PLS with the slope/intercept algorithm, thereby establishing a SSC detection model for three varieties of kiwifruit. The test result showed that this model can detect two varieties of kiwifruit precisely therein, but the precision significantly declines when the sample number is large. MOGHIMI et al. [14] utilized visible-near IR spectrum and chemometrics method to gather the spectral images within the band range of 400–1000 nm and established a PLS model that was based on the principal component analysis (PCA) by utilizing visible-near infrared spectrum and chemometrics for detecting the SSC and pH of kiwifruit. The RMSEs that correspond to the prediction set were 0.26 and 0.08. Dong et al. [15] detected the SSC of kiwifruit with the spectral images acquired within the band range of 900–1700 nm. Favorable detection results were achieved after entering the spectral band extracted into BP network with successive projection algorithm (SPA). However, this method requires massive samples. Wang et al. [16] acquired the spectral images within the band range of 1000–1800 nm and detected the SSC and pH of kiwifruit. Favorable detection performance was achieved by selecting the first-order differential PLS, but the number of samples in the prediction set will decline. Guo et al. [17] acquired the spectral images within the band range of 865.11–1711.71 nm. Moreover, the SSC of kiwifruit can be detected after entering the spectrum band extracted with the SPA into LSSVM, but the detection precision needs to be improved. Serranti et al. [18] acquired spectral images within the band range of 900–1700nm for detecting the ripeness of the plucked kiwifruit and also acquired the spectral images within the band range of 400n–1000nm for diagnosing pseudomonas infection of kiwifruit. LU et al. [19] acquired the spectral images within the band range of 408–1117 nm and reduced their dimensionality using PCA and entered into SVM. Finally, the recognition rate of the hidden damage area of kiwifruit reached up to 87.50%. HU et al. [20] acquired near-infrared spectral images to detect the hardness and SSC of kiwifruit. Favorable detection performance was achieved by utilizing the combined type spectrum pre-treatment together with PLS, but the number of samples in the prediction set was too small. MO et al. [21] acquired spectral images within the band range of 400–1000 nm and detected the SSC of apples with PLS. ElMasry et al. [22] detected the water content, the SSC, and the acidity of strawberries with full spectral band information and PLS. Attila et al. [23] extracted the chlorophyll sensitive wavelength of 678 nm as the spectral indicator to judge the ripeness of apples after studying the spectral characteristics and changes in chlorophyll, carotenoid, and water content of apple skin and flesh. Betemps et al. [24] evaluated the ripeness of apples using indexes, such as anthocyanin, flavanol, and the chlorophyll. The test showed that the chlorophyll is negatively correlated with the sugar content of apples. Noh et al. [25] detected the ripeness of apples with hyper-spectral reflection and fluorescence imaging techniques. The test result showed that its detection performance is favorable.

In summary, some research findings have been made with regard to the detection of SSC, hardness, ripeness, and other fruit parameters. However, the overall detection precision needs to be improved further, and studies on the detection of the DM of kiwifruit are limited. In this regard, an approach for extracting the spectrum characteristic that integrates uniformative variable elimination (UVE) and SPA is designed in this study so that the redundancy of the extracted low-dimensional characteristic spectral bands can be minimized. LSSVM is used as the detector, and its parameters are optimized by PSO to realize the non-destructive kiwifruit DM detection.

The remainder of the paper is organized as follows. Section III introduces the selection of experimental samples, the determination of physical and chemical values, and the acquisition of hyperspectral images. The extraction of the characteristic spectral band, the parameter optimization of the detector LSSVM, and the selection of the evaluation indexes of the detection performance are designed. Section IV compares the detection performance of different spectral band extraction methods and analyzes the test results. The final section summarizes the features of the detection method introduced in this paper and provides the conclusion.

3. METHODOLOGY

3.1. TEST SAMPLES AND PHYSICAL–CHEMICAL DETERMINATION

The test samples came from a demonstrative kiwifruit planting base in Ya'an City, Sichuan Province, China. A total of 132 green pulp kiwifruit of similar size without impairment on surface were selected. Under approximately 20 °C, the samples were numbered before gathering their hyper-spectral images and determining the physical–chemical values of their dry matter content sequentially. The water content of the kiwifruit was dried up with an IRM FD112 hot air-drying oven, and the measured dry matter content was taken as their physical–chemical values. The measurement was performed as follows. First, the petri dish was weighed as m_0, 2–5 g was taken from the middle section of the kiwifruit and placed into the petri dish and together weighed as m_1. Second, the petri dish was dried for 4 h in the drying oven at a constant temperature of 105 °C. The petri dish was taken out after drying and weighed as m_2. It was further dried for 1 h before weighing again until the difference of mass weighed before and after further drying was not greater than 0.001 g.

3.2. GATHERING AND PRE-TREATMENT OF HYPER-SPECTRAL IMAGES

The Gaia Sorter hyper-spectral imaging system (Fig. 1, supplementary material.) consists of uniform light source, spectral camera, electronically controlled mobile platform, and computer. It is powered by AC220V power source. The even light source employs four LSTS-200 bromine tungsten lamps that are arranged in trapezoidal form. The spectral camera comprises imaging spectrometer and Charge-coupled Device (CCD), and the spectral resolution is set as 2.8 nm for gathering the spectrum within the range of 400–1000 nm for 256 bands. The electrically controlled platform is used to place the kiwifruit sample, and its maximum effective loadable sample space is 300 mm×300 mm×200 mm.

The exposure time of the hyper-spectral imaging system is set to 13 s. The scanning distance is 25 cm. The advance and return speed of the electric motor is 0.4 cm/s and 1 cm/s, respectively. The images are captured when the system is stabilized. However, the captured hyper-spectral images would be mingled with partial noise information as a result of the differentiated distribution of light strength in each band, as well as the influence of the dark current noise of the camera. Thus, B&W (black and white) correction is carried out to the hyper-spectral images using the software SPEC VIEW of the hyper-spectral imaging system. The correction is performed as follows:

$$R = \frac{S - B}{W - B} \tag{1}$$

where
R—Images after correction;
W—Images of white frame;
B—Images of black frame;
S—Hyper-spectral images that are captured.

The kiwifruit regions within the B&W corrected hyper-spectral images were selected as the region of interest (ROI) by utilizing the software ENVI 5.1 (ITT Visual Information Solutions, USA).

When the hyper-spectral imaging system captures the hyper-spectral images of kiwifruit, it was susceptible to the sample state, noise, baseline drifting, and light scattering. Therefore, initial and ending noise bands should be removed from the B&W corrected ROI, and it was immediately pre-treated with multiplicative scatter correction (MSC) [9]. The full spectral band information obtained by MSC processing can eliminate the influence of scattering.

Fig. 1. Gaia sorter hyper-spectral imagining system

3.3. EXTRACTION OF CHARACTERISTIC SPECTRAL BANDS

The full spectral band information pre-treated as above was projected to low dimensional space by means of mapping or trans-formation, and then several characteristic spectral bands were extracted from the low dimensional space to represent the information of the original high-dimensional spectral bands. In this study, UVE [26] was employed to eliminate the spectral bands with less contribution to the detector. A random variable matrix was imported into the full spectral band matrix to calculate its stability. If the stability of the spectral band matrix is smaller than that of the imported random variable, then such spectral band will be eliminated as worthless information.

After screening with UVE, there were still too many characteristic spectral bands with serious collinearity. Thus SPA [15] was employed to eliminate such adverse influence. By means of vector projection analysis, SPA sought the variable group with the minimum redundant information from the spectrum matrix so as to minimize the collinearity among the variables. Suppose there are *M* samples to be detected, the spectral matrix of each sample is X_{MxJ}. The number of the column variable is *J*, $X_{k(0)}$ and *N* respectively represent the iteration vector of initial samples and the number of the extracted characteristic spectral band. The steps of SPA are as follows:

(1) Select a random column vector X_j before iteration ($n=1$) of the first time, and record as $X_{k(0)}$ ($k(0) = j$);

(2) Define the set of spectral band column vectors that haven't yet been selected $S=\{j, 1\le j \le J, j \notin \{k(0),\ldots,k(n-1)\}\}$, i.e. respectively calculate the projection of x_j on *S*:

$$P_{x_j} = x_j - (x_j^T x_{k(n-1)}) x_{k(n-1)} (x_{k(n-1)}^T x_{k(n-1)})^{-1} \quad (2)$$

(3) Solve the maximum projection in the projected vectors *k(n)*

$$k(n) = \arg(\max \| P_{x_j} \|, j \in S) \quad (3)$$

(4) Let $x_j = P_{x_j}, j \in S$;

(5) $n = n+1$, if $n < N$, then repeat the step (2)~(4).

NxJ pairs of variable groups are obtained after sequentially iterating and circulating. The Multivariable Linear Regression Model (MLR) was built for each pair of variable groups. When the RMSE of a MLR model is the minimum value, the corresponding variable group will be taken as the characteristic spectral band extracted by SPA.

3.4. DETECTOR AND ITS EVALUATION INDICATORS

LSSVM was used as the detector in this study. LSSVM substitutes the complicated secondary optimization in SVM by solving a set of linear equations and substitutes the inequation constraint in SVM optimization with equation constraint. LSSVM maps the nonlinear training samples to high dimensional linear dividable space. The kernel function of LSSVM is taken as Gaussian radial basis function, and the detection performance of LSSVM is greatly affected by parameters (γ, δ^2), of which γ is the regularized parameter of LSSVM and δ^2 is the kernel parameter within the radial basis function. The LSSVM model is expressed as follows:

$$\mathrm{y(x)} = \sum_{\mathrm{k}=1}^{\mathrm{n}} \mathrm{a_k K(x, x_k) + b} \quad (4)$$

where
$y(x)$ — Output value of LSSVM;
$K(x,x_k)$ — Kernel matrix;
x_k— Input variable;
a_k— Lagrange multiplier;
b— Model bias.

3.4.1. Optimization of detector

γ and δ^2 were optimized with PSO [27]. As a global random search algorithm, PSO evaluates the fitness of each particle and updates the optimal position and the optimal global position of the current particle. The optimal values of γ and δ^2 can be obtained after iterating for multiple times. The fitness of the particles is related to the RMSE of the detector. The smaller the RMSE is, the greater the particle fitness would be, and the stronger the fitness of such particle is.

The solution space of the problem to be searched is set to D, and the number of particle swarms is N. The velocity and the position of ith particle is $V_i = (v_i^{(1)}, v_i^{(2)}, \ldots v_i^{(D)})$ and $X_i = (x_i^{(1)}, x_i^{(2)}, \ldots x_i^{(D)})$, and the optimal position of such particle and particle group that has been researched is $P_i = (p_i^{(1)}, p_i^{(2)}, \ldots p_i^{(D)})$ and $P_g = (p_g^{(1)}, p_g^{(2)}, \ldots p_g^{(D)})$. Then, the computational formulas for the velocity and the position of each particle are expressed as follows:

$$v_i^{(d)}(i+1) = w \times v_i^{(d)}(i) + c_1 \times \lambda_1 \times \left(p_i^{(d)}(i) - x_i^{(d)}(i) + c_2 \times \lambda_2 \times \left(p_g^{(d)}(i) - x_i^{(d)}(i)\right)\right) \quad (5)$$

$$x_i^{(d)}(t+1) = x_i^{(d)}(t) + v_i^{(d)}(t+1) \quad (6)$$

where W is the inertia factor, and i is the present times of iteration,$1 \le i \le N$, and $1 \le d \le D$. c_1 and c_2 are constants greater than 0. λ_1 and λ_2 are random digits between 0 and 1.

3.4.2. Selection of detection performance evaluating indicators

Root mean square errors of calibration (RMSE) and R were taken as indicators for LSSVM performance evaluation, and they were calculated as follows:

$$R = \frac{\sqrt{\sum_{i=1}^{n} (\bar{y}_i - y_i)^2}}{\sqrt{\sum_{i=1}^{n} (\bar{y}_i - y)^2}} \quad (7)$$

$$RMSE = \sqrt{\frac{\sum_{i=1}^{n} (\bar{y}_i - y_i)^2}{n}} \quad (8)$$

where
R, *RMSE*— Correlation coefficient of calibration and root mean square errors of calibration;
y— Mean value of the detected physical-chemical value of the DM of kiwifruit samples;
$\bar{y}_i$— Non-destructive detection value of the ith kiwifruit sample;
n— The number of kiwifruit samples to be detected.

RMSE reflects the deviation between the non-destructive detection value of the DM of kiwifruit and its physical–chemical detection value. The smaller this value is, the smaller the deviation is. R reflects the fitting degree between the non-destructive detection value of the DM of kiwifruit and its physical–chemical detection value. The closer the fitting degree to 1 is, the more the detection precision of the LSSVM is.

4. RESULT ANALYSIS AND DISCUSSION

4.1. DETECTION RESULT OF PHYSICAL-CHEMICAL VALUE

A total of 132 kiwifruit samples were divided into a training set and a prediction set by utilizing the sample set partitioning based on joint X-Y distance (SPXY), of which 90 and 42 samples were found in the training and prediction sets, respectively. All physical–chemical detection values of the DM of kiwifruit sample were listed in Table 1.

Sample set	Sample qty	Min. value	Max. value	Mean value	Std. deviation
T. set	90	13.10	18.00	15.42	1.48
P. set	42	13.60	17.40	15.47	1.11

Table I. Physical–chemical detection value of the DM of kiwifruit (%)

4.2. RESULTS OF SPECTRAL BANDS PRE-TREATMENT

The hyper-spectral images of 132 kiwifruit samples were obtained from the spectral band range of 400–1000 nm. After carrying out B&W correction, the kiwifruit regions therein were selected as ROI with software ENVI 5.1. The hyper-spectral image of ROI of a kiwifruit sample was shown as Fig. 2.

Fig. 2. Hyperspectral image of ROI

The hyper-spectral image of ROI of each kiwifruit contained 256 original spectral bands, and the corresponding hyper-spectral curve was shown as Fig. 3(a). According to Fig. 3(a), noise was found on the initial and ending spectral bands in the hyper-spectral curve. Thus, 217 full spectral bands remained after eliminating the initial and ending spectral bands. Then, the information of the 217 full spectral bands was pre-treated, and the curve of the pre-treated 217 full spectral bands was shown as Fig. 3(b).

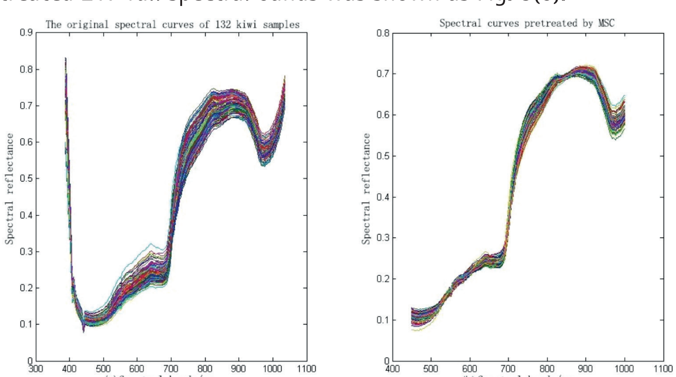

Fig. 3. Original spectral curve of ROI of kiwifruit and its pre-treatment

4.3. EXTRACTION RESULT OF CHARACTERISTIC SPECTRAL BANDS

The MSC pre-treated full spectral bands had large data size and strong redundancy. Thus, UVE was used to screen the spectral bands. A total of 217 full spectral bands in Fig. 3(b) were screened with UVE, and the number of vectors imported with random vector matrix was also 217.

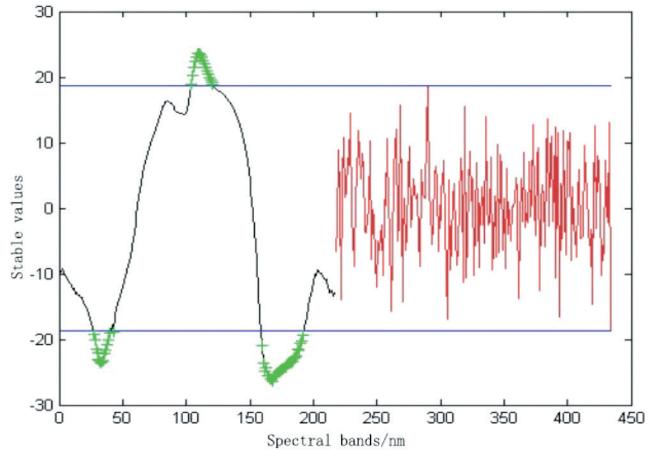

Fig.4 . Distribution curve of UVE stability values

The left curve (black) in Fig. 4 corresponds to the stable value curve of 217 full spectral bands, and the right curve (red) in Fig. 4 refers to the stable value curve of the 217 random variables that was imported. The two horizontal lines determined by the stable values of random variables indicated the screening of the threshold value of the spectral bands. Moreover, the spectral bands between the horizontal lines were all deleted as uninformed variables, whereas the spectral bands beyond the horizontal lines were preserved, that is, UVE extracts 66 characteristic spectral bands from 217 full spectral bands. According to Fig. 4, 69.59% of the 217 spectral bands were deemed as uninformed variables.

A part of the 66 characteristic spectral bands extracted by UVE were overlapped in the spectral band regions (i.e., collinearity was observed among spectral bands, and then SPA was employed immediately to eliminate the collinearity among the 66 characteristic spectral bands. When the RMSE of a MLR model was at the minimum value, the variable group that corresponds to such MLR model was then deemed as the characteristic spectral band extracted by SPA. In the process of SPA extraction, when the RMSE was the minimum value (i.e., 0.510), SPA extracted five characteristic spectral bands that were 781.84, 792.17, 820.66, 864.98, and 884.08 nm. Subsequently, the number of spectral band reduced by 92.42% over the 217 spectral bands. Five characteristic spectral bands entered into the LSSVM for training, thereby optimizing their parameters and finishing the DM detection of kiwifruit.

4.4. DETECTION RESULT OF LSSVM

In Formula (5), set $c_1 = c_2$=2, the initial value of inertia factor was set as 0.9, the maximum iteration times was set as 100, the initial number of particle population was set as 20, the optimizing range of γ was set as [0.01,300], and the optimizing range of δ^2 was set as [0.01,200]. LSSVM was trained with different characteristic spectral bands, and the values of γ and δ^2 optimized by PSO was shown as Table 2. In this table, the greater γ indicates the lower the allowable error of LSSVM, whereas the smaller δ^2 indicates the higher the LSSVM detection precision.

According to Table 2, LSSVM was trained using the five characteristic spectral bands that were extracted with UVE+SPA, and

CSB (Characteristic spectral band)	Number of CSB	γ	δ^2
Full spectral bands	217	259.20	25.41
UVE	66	263.21	18.72
UVE+SPA	5	280.54	11.45

Table II. Parameters γ and δ^2 optimized by PSO

the optimal parameter values γ=280.54, δ^2=11.45 were obtained after PSO optimizing. The trained LSSVM has better detection precision, which was superior to the detection performance of LSSVM that were trained with the 217 full spectral bands and the 66 characteristic spectral bands extracted with UVE. Of course, the detection performance of LSSVM trained with the 217 full spectral bands was the most inferior. The relationship between the DM detection value of LSSVM undergone three types of characteristic training to the training set and its corresponding physical–chemical detection value was shown as Fig. 5.

Table 3 showed that when UVE+SPA+LSSVM was employed, the detection evaluation indicators for the training set were R=0.91, RMSE=0.28, and that for the prediction set were R=0.89, RMSE=0.31. According to comparison, the detection performance of this method, with features of small detection error and high degree of fitting, was superior to the other two methods no matter with regard to the training set or the prediction set. The detection performance of UVE+LSSVM came to the second, and the detection performance of full spectral bands + LSSVM was the most inferior. That the detection performance of UVE+SPA+LSSVM was superior to UVE+LSSVM indicated that the collinearity among the characteristic spectral bands reduced the detection precision of LSSVM, while such collinearity can be effectively eliminated by SPA. That the detection performance of UVE+LSSVM was superior to that of full spectral bands + LSSVM indicated that the redundancy of full spectral bands reduced the detection precision of LSSVM.

The results of detecting the DM of the prediction set with UVE+SPA+LSSVM were shown in Fig. 6. According to Fig. 6, the

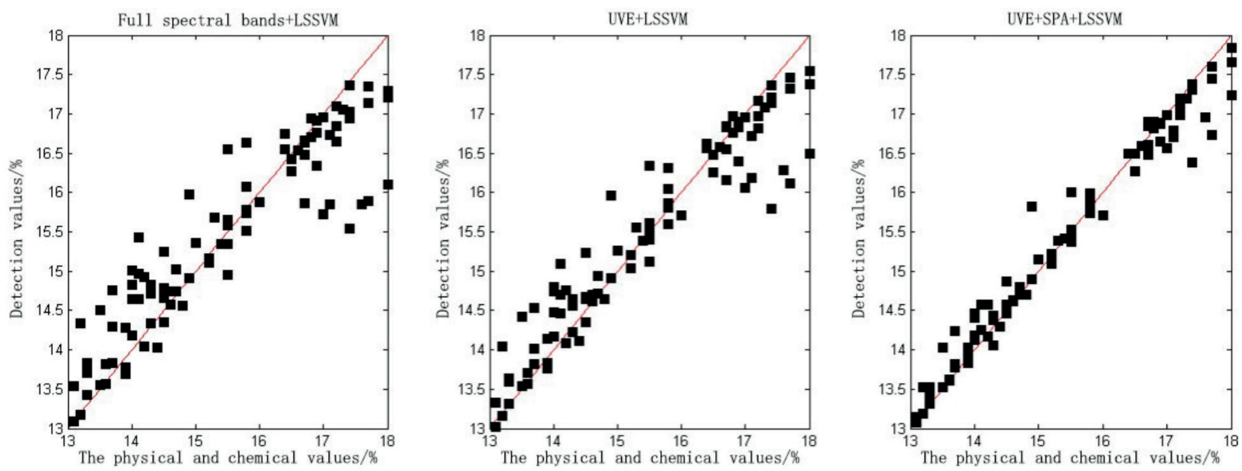

Fig. 5. Relationship between the DM detection value of LSSVM to the training set and its physical-chemical determination value

Fig. 5 showed the relationship between the physical–chemical determination value of the DM (horizontal axis) of training set and the detection value of the DM (vertical axis). All DM detection values of LSSVM to the training set were located on both sides of the regression line, but they vary in distribution: the training result of UVE+SPA+LSSVM was the best. At this point, the DM detection values of LSSVM were in apparent linear relationship with the physical–chemical determination values, which indicated that the characteristic spectral bands extracted with UVE+SPA can reflect the DM of the training set best (Fig. 5(c)). The training result of UVE+LSSVM was the second. The linear relationship between the detection values of LSSVM and the physical–chemical values slightly declined (Fig. 5(b)). However, the training result of full spectral bands + LSSVM was the most inferior. At this point, the DM detection values of LSSVM were most dispersedly distributed (Fig. 5(a)).

The DM of the training set and that of the prediction set were detected using the trained LSSVM and evaluated with the aforementioned indicators. Table 3 shows the results.

Detection method	Training set		Prediction set	
	RMSE	R	RMSE	R
Full spectral band +LSSVM	0.63	0.79	0.74	0.74
UVE+ LSSVM	0.50	0.83	0.66	0.75
UVE+SPA+LSSVM	0.28	0.91	0.31	0.89

Table III. Comparison of detection results

linear relationship between the physical–chemical detection values of the DM of the prediction set and DM detection values of LSSVM favorable. Thus, this method can also detect the DM of the test set effectively.

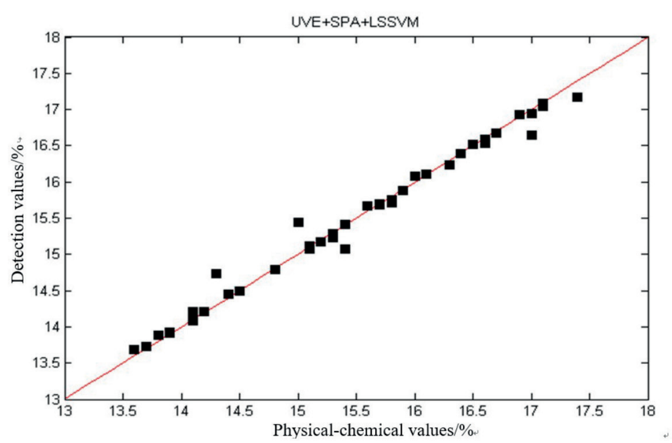

Fig. 6.DM detection results of UVE+SPA+LSSVM to the prediction set

5. CONCLUSIONS

To detect the DM of kiwifruit in a non-destructive way with hyper-spectral images and seek a method for extracting the characteristic spectral bands that can best reflect the DM of kiwifruit, this study analyzed the full spectral bands of the hyper-spectral images intensively after having them pre-treated, and a feasible non-destructive detection method has been designed. The following conclusions were obtained through research:

(1) The influence of spectral scattering can be eliminated by pre-treating the hyper-spectral images of kiwifruit with MSC effectively.

(2) The redundancy of full spectral bands can be reduced by screening out a part of spectral bands from full spectral bands with UVE. SPA is employed immediately to eliminate the collinearity among the spectral bands and reduce the calculating load of LSSVM.

(3) The optimal γ and δ^2 can be obtained by optimizing LSSVM with PSO, which is helpful for improving the kiwifruit DM detection precision of LSSVM.

An UVE+SPA+LSSVM detection method was designed in this study by integrating the pre-treatment of hyper-spectral images and characteristic band selection. According to the test results, this method is an effective and practical way with higher precision for non-destructive detection, and it can be also applied to detect the DM of other fruits, such as citrus fruits, with equal utility. The detection precision of this method can certainly be improved further, and the detection samples are also limited to one variety of kiwifruit. Next, it would be able to detect multiple internal parameters of multiple varieties of kiwifruit and further optimize the characteristic extraction process.

REFERENCES

[1] Zhang JY, Mo ZH, Huang SN. Development of kiwifruit industry in the world and analysis of trade and international competitiveness in China entering 21st century.Chinese Agriculture Science Bulletin. November 2014.Vol. 30-23.p. 48-55. DOI: http://dx.doi.org/10.11924/j.issn.1000-6850.2013-2887

[2] Qiu JH. Study on the cultivation technology of Kiwifruit. Horticulture seed industry. June 2017.Vol. 35-06.p.82-85.

[3] Gao S, Wang QH. Comprehensive detection of internal quality of red globe grape extract based on near infrared spectroscopy. Chinese Journal of luminescence.December 2019. Vol.40-12.p.1574-1584. DOI: http://dx.doi.org/10.3788/fgxb20194012.1574

[4] Jie DF, Li ZH, Zhao JW, et al. Visualized detection of soluble solid content distribution of navel orange based on hyperspectral diffuse transmittance imaging. Chinese Journal of luminescence. May 2017. Vol. 38-5. p. 685-691. DOI: http://dx.doi.org/10.3788/fgxb20173805.0685

[5] Leiva-valenzuela GA, Lu R, Aguilera JM. Assessment of internal quality of blueberries using hyperspectral transmittance and reflectance images with whole spectra or selected wavelengths. Innovative Food Science and Emerging Technologies. August 2014. Vol. 24-8. p. 2-13. DOI: http://dx.doi.org/10.1016/j.ifset.2014.02.006

[6] Kranjcic N, Zupan R, Rezo M. Satellite-based hyperspectral imaging and cartographic visualization of bark beetle forest damage for the city of Cabar. Tehnicki Glasnik-Technical Journal. March 2018.Vol.12-1.p.39-43. DOI: http://dx.doi.org/10.31803/tg-20171219085721

[7] Lam CT, Chan PH, Lee PS, et al. Chemical and biological assessment of Jujube (Ziziphus jujuba)-containing herbal decoctions: induction of erythropoietin expression in cultures. Journal of Chromatography B. July 2016. Vol. 1026-7. p. 254-262. DOI: http://dx.doi.org/10.1016/j. jchromb.2015.09.021

[8] Das B, Sahoo RN, Pargal S, et al. Quantitative monitoring of sucrose, reducing sugar and total sugar dynamics for phenotyping of water-deficit stress tolerance in rice through spectroscopy and chemometrics. Spectrochimica Acta Part A: Molecular and Biomolecular Spectroscopy. March 2017.Vol. 192-3.p. 41-51. DOI: http://dx.doi.org/10.1016/j.saa.2017.10.076

[9] Santagapita PR, Tylewicz U, Panarese V, et al. Non-destructive assessment of kiwifruit physico-chemical parameters to optimise the osmotic dehydration process: a study on FT-NIR spectroscopy. Biosystems Engineering. February 2016.Vol. 142. p. 101-109. DOI: http://dx.doi.org/10.1016/j. biosystemseng.2015.12.011

[10] He CL, Wang J, Lai SY, et al. Image fusion in remote sensing based on spectral unmixing and improved non - negative matrix factorization algorithm. Journal of Engineering Science and Technology Review. March 2018.Vol.11-3. p.79-88. DOI: http://dx.doi.org/10.25103/jestr.113.11.

[11] Li M, Pullanagari RR, Pranamornkith T, et al. Quantitative prediction of post storage 'Hayward' kiwifruit attributes using at harvest Vis-NIR spectroscopy. Journal of Food Engineering. June 2017.Vol. 202-06.p. 46-55. DOI: http://dx.doi.org/10.1016/j.jfoodeng.2017.01.002

[12] Mcglone VA, Clark CJ, Jordan RB. Comparing density and VNIR methods for predicting quality parameters of yellow-fleshed kiwifruit (Actinidia chinensis). Postharvest Biology Technology. January 2007.Vol. 46-1.p. 1-9. DOI: http://dx.doi.org/10.1016/j.postharvbio.2007.04.003

[13] Li QQ, Liu DY, Yang B, et al. Application of Slope/Bias Algorithm in Portable Detection of Contents of Soluble Solids of Kiwifruit. Food Science. July 2018.Vol. 39-14.p. 257-262. DOI: http://dx.doi.org/10.7506/spkx1002-6630-201814038

[14] Moghimi.A, Aghkhani MH, Sazgarnia A, et al. Vis/NIR spectroscopy and chemometrics for the prediction of soluble solids content and acidity (pH) of kiwifruit. Biosystems Engineering. March 2010.Vol. 106-3.p. 295-302. DOI: http://dx.doi.org/10.1016/j.biosystemseng.2010.04.002

[15] Dong JL, Guo WC. Nondestructive detection on soluble solids content of postharvest kiwifruits based on hyperspectral imaging technology. Food Science. August 2015.Vol. 36-16.p. 101-106. DOI: http://dx.doi.org/10.7506/spkx1002-6630-201516018

[16] Wang X, Song QH. Detecting of soluble solid content and PH of kiwifruit by near-infrared spectroscopy. The Food Industry. March 2017.Vol. 38-3.p.305-307.

[17] Guo WC, Zhao F, Dong JL. Nondestructive measurement of soluble solids content of kiwifruits using near-Infrared hyperspectral imaging. Food Analytical Methods. January 2016.Vol. 9-1.p.38-47. DOI: http://dx.doi.org/10.1007/s12161-015-0165-z

[18] Serranti S, Bonifazi G, Luciani V. Non-destructive quality control of kiwifruits by hyperspectral imaging. Society of Photo-Optical Instrumentation Engineers Commercial + Scientific Sensing and Imaging. May 2017. Vol.10217.p.1205-1212. DOI: http://dx.doi.org/ 10.1117/12.2255055

[19] Lue Q, Tang MJ, Cai JR, et al. Vis/NIR hyperspectral imaging for detection of hidden bruises on kiwifruits. Czech Journal of Food Sciences. September 2011.Vol. 6-29.p. 595-602. DOI: http://dx.doi.org/10.1080/19476337.2011.616959

[20] Hu XF, Lin M, Liu HJ, et al. Nondestructive testing of kiwifruit quality by near infrared diffuse reflectance spectroscopy. Physical and chemical test - Chemical volume. January 2018.Vol. 54-1.p.8-12. DOI: http://dx.doi.org/10.11973/lhjy-hx201801002

[21] Mo C, Kim MS, Kim G, et al. Spatial assessment of soluble solid contents on apple slices using hyperspectral imaging. Biosystems Engineering. July 2017.Vol. 159. p. 10-21.DOI: http://dx.doi.org/10.1016/j.biosystemseng.2017.03.015

[22] ElMasry G, Wang N, ElSayed A, et al. Hyperspectral imaging for nondestructive determination of some quality attributes for strawberry. Journal of Food Engineering. January 2007.Vol.81-1.p.98-107. DOI: http://dx.doi.org/10.1016/j.jfoodeng.2006.10.016

[23] Attila N, Peter R, Janos T. Spectral evaluation of apple fruit ripening and pigment content alteration. Scientia Horticulturae. March 2016.Vol. 201-3.p.256-264.DOI: http://dx.doi.org/10.1016/j.scienta.2016.02.016

[24] Betemps DL, Fachinello JC, Galarca SP, et al. Non-destructive evaluation of ripening and quality traits in apples using a multiparametric fluorescence sensor. Journal of Science and Food Agriculture. January 2012.Vol. 92-1.p.1855-1864.DOI: http://dx.doi.org/10.1002/jsfa.5552

[25] Noh HK, Peng YK, Lu RF. Integration of hyperspectral reflectance and fluorescence imaging for assessing apple maturity. Transactions of The American Society of Agricultural and Biological Engineers. March 2007.Vol. 50-3.p. 963-971.DOI: http://dx.doi.org/10.13031/2013.23119

[26] Liu YD, Xiao HC, Sun XD, et al. Spectral feature selection and discriminant model building for citrus leaf Huanglongbing. Transactions of the Chinese Society for Agricultural Engineering. March 2018.Vol. 34-3.p. 180-187.DOI: http://dx.doi.org/10.11975/j.issn.1002-6819.2018.03.024

[27] Li L, Gao LF, Zhao SJ. Question of SVM kernel parameter optimization with particle swarm algorithm based on neural network. Computer Engineering and Applications. April 2015.Vol. 51-4.p.162-164.DOI: http://dx.doi.org/10.3778/j.issn.1002-8331.1304-0338

APPRECIATION

This study was supported by the natural science program of sichuan education departmen under Grant No.17ZB0333 and the Ya'an City-school partnership program under Grant No. 2018sxhz02.